Generalized Paschen's Curves for Extraterrestrial Atmospheric Electricity

J. A. Riousset[1] (jriousset@fit.edu), Jared P. Nelson[1], Joshua Mendez-Harper[2], Annelisa B. Esparza[1], Josef Dufek[2], & Jack Zhije Chen[1]

1: Aerospace, Physics & Space Sciences Department, Florida Institute of Technology, Melbourne, FL

2: Earth Sciences Department, University of Oregon, Eugene, OR

Abstract

In *Riousset et al.* (2020), we investigate putative and confirmed lightning events in the solar system by comparing the conventional breakdown threshold, E_k, in three planetary atmospheres (Earth, Mars, and Venus). The study shows how minor active components can dramatically reduce E_k locally. It further confirms the role of environmental factors (e.g., atmospheric composition) in facilitating the initiation of atmospheric discharges. Here, we continue this work through a study of the importance of geometrical factors in the sustainability of *Townsend*'s (1900) discharges. The widely accepted *Paschen*'s (1889) law describes these events as non-thermal, self-sustained discharges occurring in high voltage, low current, and low-pressure conditions between two parallel plate electrodes (e.g., *Raizer*, 1997). This paper develops a new formalism adapted to cylindrical and spherical geometries and an experimental setup for its validation. We demonstrate how a simple change in the geometry results in equations requiring numerical solutions and transforming the Paschen's curves and Stoletov's points into surfaces and curves, respectively. We compare our work to the peer-reviewed literature and in-house experiments and explore the impact on modeling initiation and propagation of discharges in non-Earth-like environments. Lastly, we conclude on the role of such studies for risk assessments in planetary exploration.

I. Introduction

Figure 1: Hypothesized origin of Martian electrical activity (*Yair*, 2012).

E_c: Thermal runaway breakdown.
E_k: Conventional breakdown field.
E_{cr}^{+}: Positive streamer propagation threshold.
E_{cr}^{-}: Negative streamer propagation threshold.
E_t: Relativistic runaway field.
E_ℓ: Leader propagation threshold.

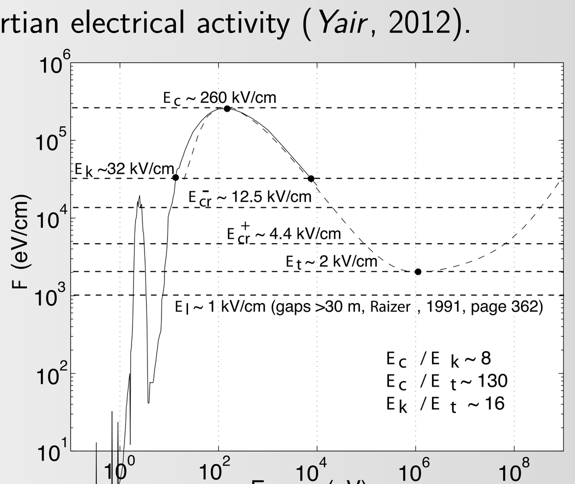

Figure 2: ▶ Electrical discharge thresholds in air (*Pasko*, 2006).

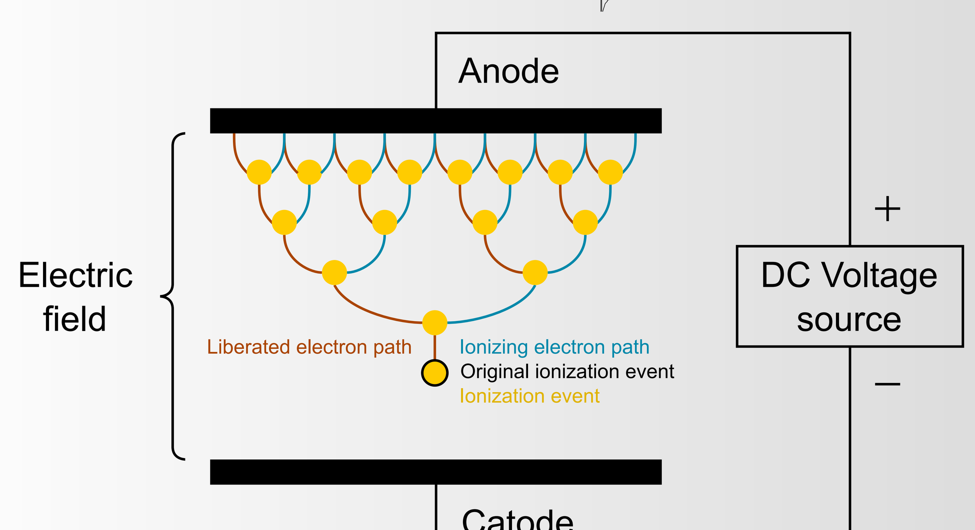

Figure 3: Principle of *Townsend*'s (1900) discharge (Wiki).

II. Model Formulation

II.a Geometry

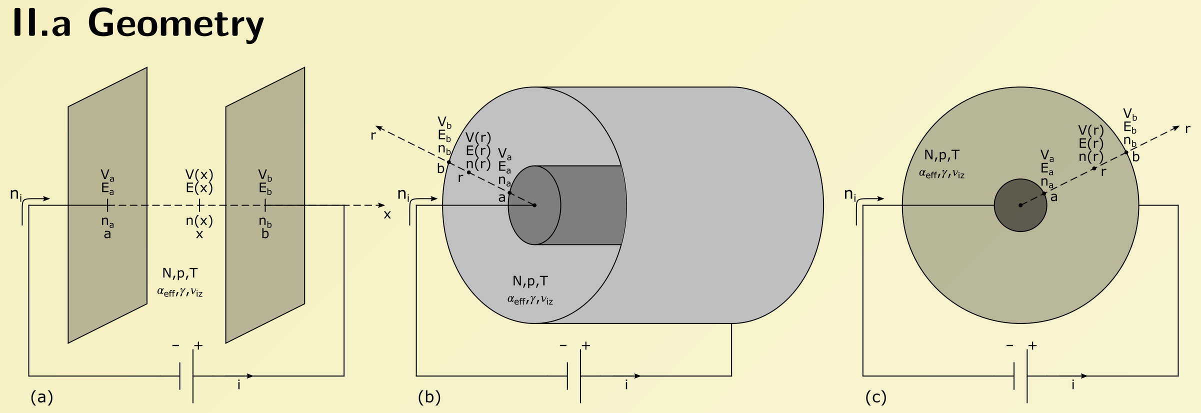

Figure 4: Townsend's discharge in 1-D geometries: (a) Parallel plates (Cartesian); (b) Coaxial cylindrical electrodes; (c) Concentric spherical electrodes. The gap between the electrodes contains a gas with the number density N ($\mathrm{m^{-3}}$) at temperature T (K), under the pressure p (Pa). The avalanche is characterized by the Townsend effective ionization coefficient $\alpha_{\rm eff}$ ($\mathrm{m^{-1}}$), the secondary ionization coefficient γ, and effective ionization frequency $\nu_{\rm iz}$ ($\mathrm{s^{-1}}$). The quantities n_i, n_a, $n(r)$, $n(x)$, and n_b correspond to the electron density in $\mathrm{m^{-3}}$ carried by the electronic current i, emitted from the cathode at a, measured at a point r or x between the electrodes a and b, and received at the anode at b, respectively. The corresponding electric potential and field are denoted V (V) and E (V/m).

II.b Electric Fields

$$\nabla \cdot \vec{E} = 0 \Rightarrow \boxed{E(r) = E_a \left(\frac{a}{r}\right)^{\delta}} \qquad (1)$$

where $\delta = 0$, 1, and 2 for the Cartesian, cylindrical, and spherical 1-D geometries displayed in Figures 4a, 4b, and 4c, respectively.

II.c Scaling

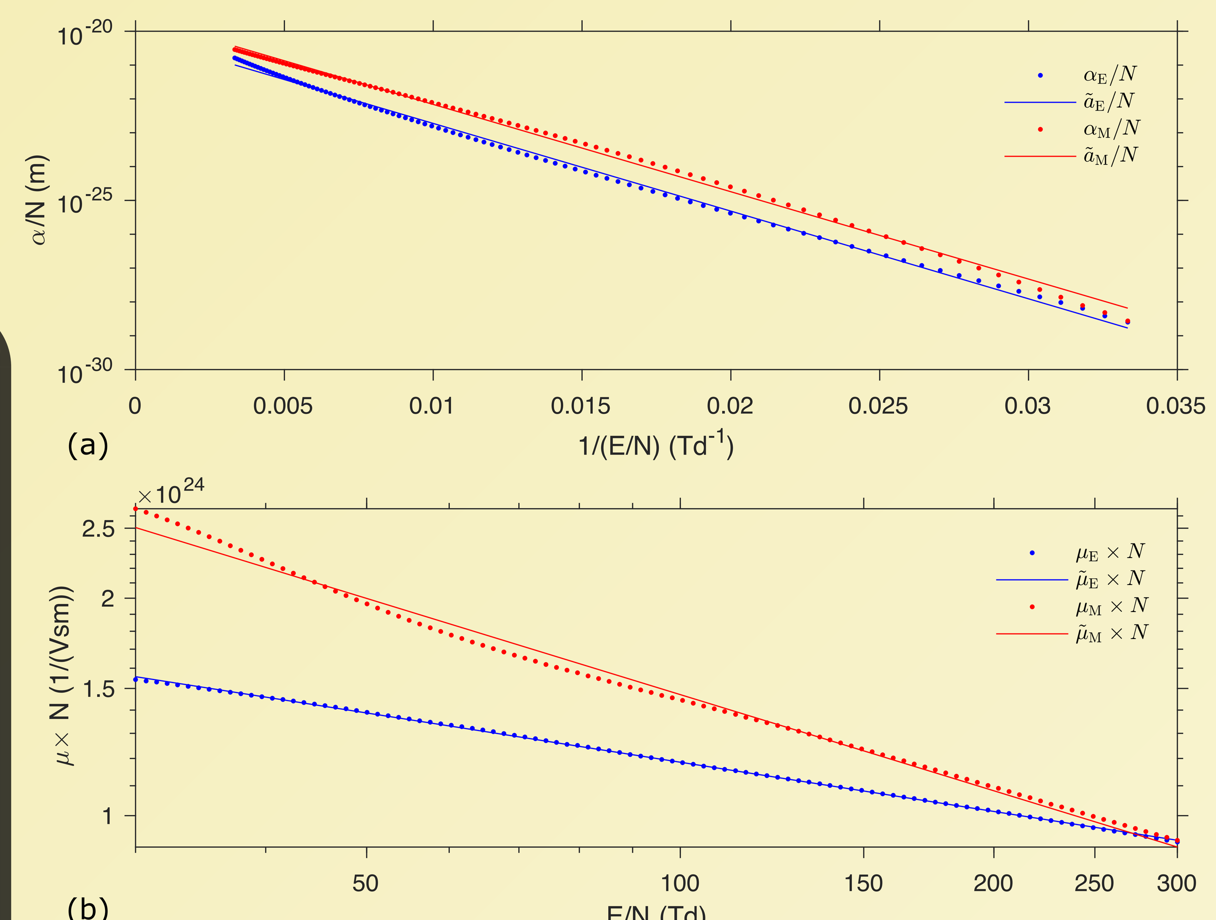

Figure 5: Scaling laws for (a) the reduced effective Townsend ionization coefficient α/N and (b) reduced mobility $\mu \times N$ plotted against the reduced electric field E/N. Blue and red colors correspond to Earth and Mars-like atmospheres, respectively (see Table 1).

		Earth	Mars
Molar fraction	Ar	9.05×10^{-3}	1.60×10^{-2}
	CO	1.84×10^{-7}	≈ 0
	CO_2	3.79×10^{-3}	95.7×10^{-2}
	He	5.04×10^{-6}	≈ 0
	N_2	75.68×10^{-2}	2.7×10^{-2}
	N_2O	3.43×10^{-7}	≈ 0
	O_2	20.30×10^{-2}	≈ 0
	O_3	3.01×10^{-8}	≈ 0
	T_g	273.04 K	231.2 K
	N	$2.688 \times 10^{25}\,\mathrm{m^{-3}}$	$1.889 \times 10^{23}\,\mathrm{m^{-3}}$
Coefficients	A	$7.36 \times 10^{-21}\,\mathrm{m^2}$	2.62×10^{-20}
		2.60 /(cm Torr)	10.95 /(cm Torr)
	B	596.8 Td	594.3 Td
		211.1 V/(cm Torr)	248.2 V/(cm Torr)
	C	3.36×10^{24} /(Vms)	1.13×10^{25} /(Vms)
	D	−0.265	−0.442

Table 1: Input parameters for BOLSIG runs. Atmospheric parameters are from NASA's Global Reference Atmospheric Models (GRAMs) (EarthGRAM by *Leslie* (2008) and Mars-GRAM by *Justh et al.* (2010)) taken at the surface $z = 0\,\mathrm{km}$ on January 1st, 2000, at 1200 UT, at 0° latitude and 0° longitude. These are the same surface conditions as in (*Riousset et al.*, 2020). Values A, B, C, D define the approximations for the reduced Townsend ionization coefficient $\frac{\tilde{\alpha}}{N} = A \exp\left(-\frac{B}{E/N}\right)$, and reduced mobility $\tilde{\mu} \times N = C\left(\frac{E}{N}\right)^{D}$.

II.d Avalanching

$$\boxed{\frac{\partial n}{\partial t} + \nabla \cdot n\vec{u} = n\nu_{\rm iz}} \Rightarrow \frac{\mathrm{d}\ln\left(r^{\delta} n(r)\mu(E(r))E(r)\right)}{\mathrm{d}r} = \alpha_{\rm eff}(E(r)) \qquad (2)$$

with $\delta = 0$, 1, and 2 for the Cartesian, cylindrical, spherical cases (Figure 4).

$$A_{\rm av} \triangleq \frac{n_b}{n_a} = \frac{\mu(E_a)}{\mu(E_b)} \exp\left(\int_a^b \alpha_{\rm eff}(E)\,\mathrm{d}r\right)$$

$$\left.\begin{aligned} n_a &= n_i + n_\gamma \\ n_\gamma &= \gamma(n_b - n_a) \\ n_b &= A_{\rm av} n_a \end{aligned}\right\} \Rightarrow \boxed{\frac{n_b}{n_i} = \frac{\frac{A_{\rm av}}{\gamma}}{1 + \frac{1}{\gamma} - A_{\rm av}}} \qquad (3)$$

Self-Sustaining Condition

From (3):

$$A_{\rm av} = 1 + \frac{1}{\gamma} \Rightarrow \boxed{\int_a^b \alpha_{\rm eff}(E)\,\mathrm{d}r + \ln\left(\frac{\mu(E_a)}{\mu(E_b)}\right) = \ln\left(1 + \frac{1}{\gamma}\right)} \qquad (4)$$

From the fits in Table 1:

$$\int_a^b A N e^{-\frac{B}{E_a/N}\left(\frac{r}{a}\right)^{\delta}}\,\mathrm{d}r + D\ln\left(\left(\frac{b}{a}\right)^{\delta}\right) = \ln\left(1 + \frac{1}{\gamma}\right)$$

$$\boxed{\int_0^d A p e^{-\frac{B}{E_a/p}\left(1+\frac{p\ell}{pa}\right)^{\delta}}\,\mathrm{d}\ell + D\ln\left(\left(1 + \frac{pd}{pa}\right)^{\delta}\right) = \ln\left(1 + \frac{1}{\gamma}\right)} \qquad (5)$$

III. Results

III.a Theory

Critical Electric Fields:

$$e^{-\frac{Bp}{E_a}} = \frac{1}{Apd}\ln\left(1 + \frac{1}{\gamma}\right), \quad \delta = 0 \qquad (6a)$$

$$-\frac{E_a}{Bp}\left[\exp\left(-\frac{Bp}{E_a}\left(1 + \frac{pd}{pa}\right)\right) - \exp\left(-\frac{Bp}{E_a}\right)\right] = \frac{1}{Apa}\ln\left(\frac{\left(1 + \frac{1}{\gamma}\right)}{\left(1 + \frac{pd}{pa}\right)^{D}}\right), \quad \delta = 1 \qquad (6b)$$

$$\sqrt{\frac{E_a}{Bp}}\left[\mathrm{erf}\left(\sqrt{\frac{E_a}{Bp}}\left(1 + \frac{pd}{pa}\right)\right) - \mathrm{erf}\left(\sqrt{\frac{E_a}{Bp}}\right)\right] = \frac{2}{\sqrt{\pi}}\frac{1}{Apa}\ln\left(\frac{\left(1 + \frac{1}{\gamma}\right)}{\left(1 + \frac{pd}{pa}\right)^{2D}}\right), \quad \delta = 2 \qquad (6c)$$

Critical Voltages:

$$V_{\rm cr} = \begin{cases} \frac{E_a}{p} pa \ln\left(1 + \frac{pd}{pa}\right) & \delta = 1 \\ \frac{E_a}{p} pa \frac{\left(1 + \frac{pd}{pa}\right)^{1-\delta} - 1}{1 - \delta} & \delta \in \{0, 2\} \end{cases} \qquad (7)$$

von Engel and Steenbeck's (1932; 1934) solution for parallel plate electrodes (Figure 4a):

$$V_{\rm cr} = \frac{Bpd}{\ln\left(\frac{Apd}{\ln\left(1 + \frac{1}{\gamma}\right)}\right)} \qquad (8)$$

III.b Earth

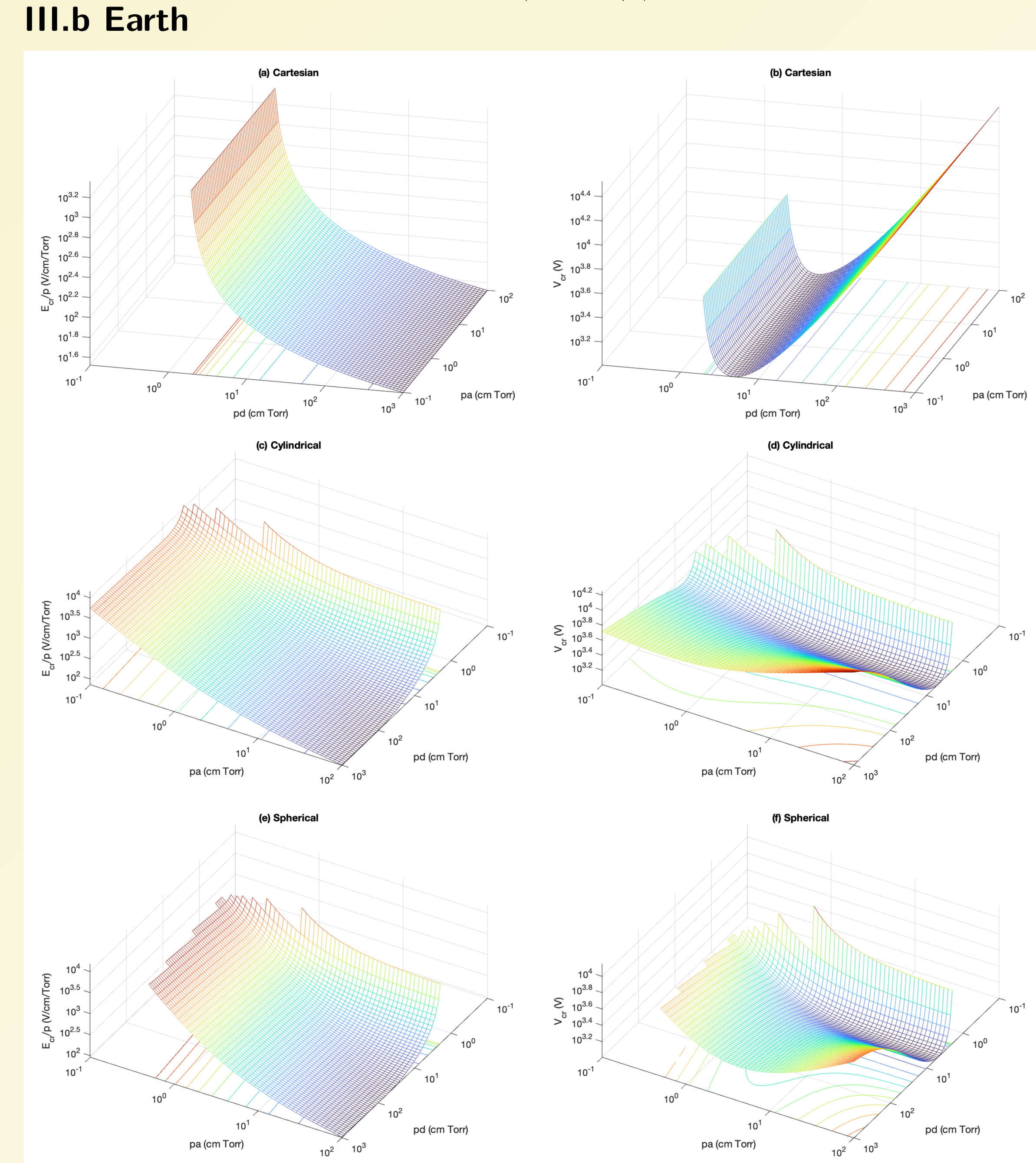

Figure 6: Reduced critical electric field $E_{\rm cr}$ (left column) and potential $V_{\rm cr}$ (right) column) as a function of the reduced characteristics length of electrode a and distance d between electrodes a and b for Earth. (a), (b): Parallel geometries; (c), (d): Coaxial geometries; (e), (f) Concentric spherical electrodes.

III.c Mars

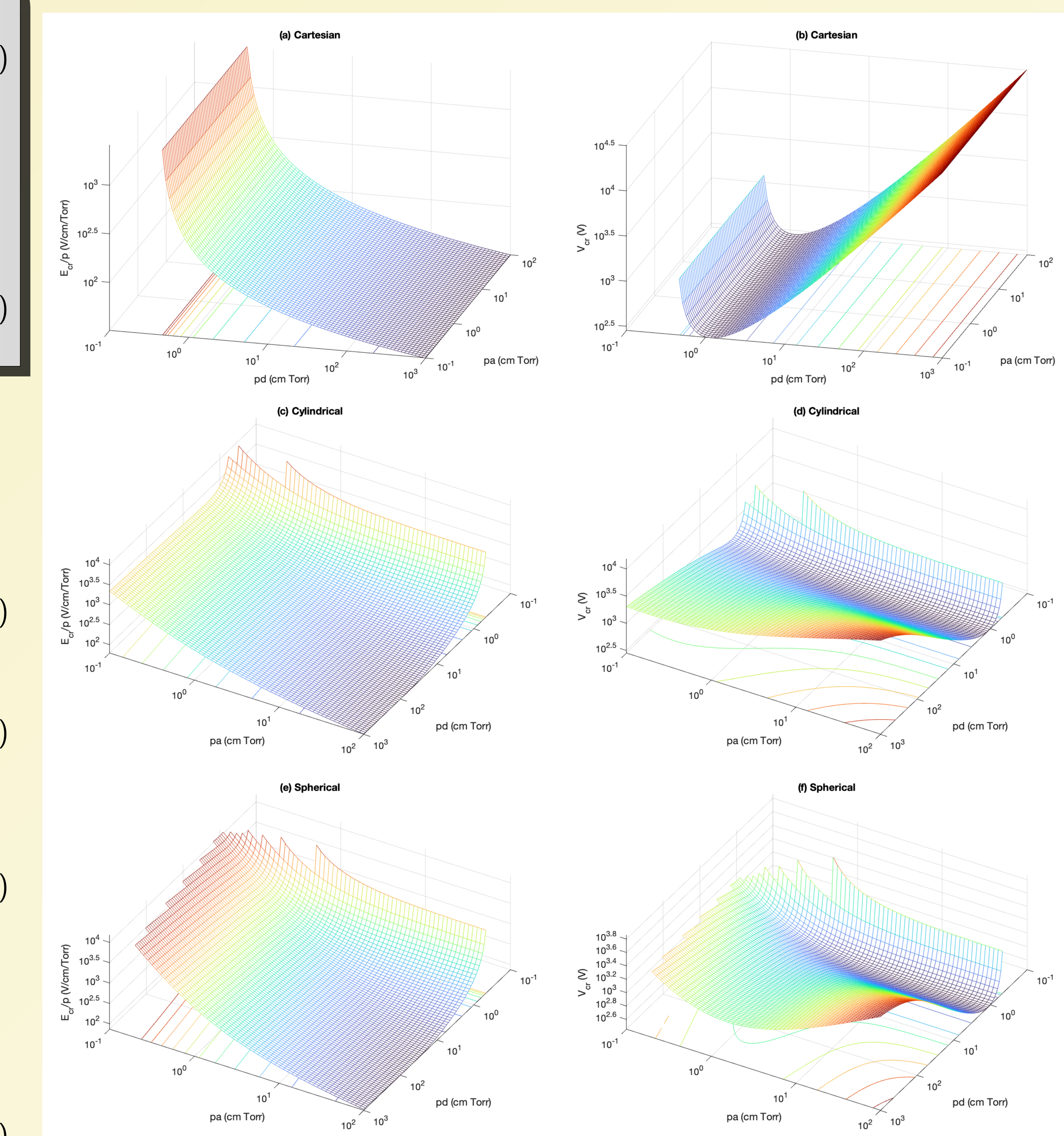

Figure 7: Same as Figure 6 for Mars.

IV. Conclusions

The principal results and contributions from this work can be summarized as follows:

1. We propose a generalization of *Townsend*'s (1900) theory applicable to parallel-plate, coaxial cylindrical, and concentric spherical electrodes. Numerical modeling lets us solve the conditions of self-sustainability in the new geometries.
2. The new condition of self-sustainability requires that the reduced mobility approximately follows a power law. We calculate its coefficients for Earth and Mars atmospheric conditions.
3. For non-planar geometries, the critical electric field and potential depend on the distance between the electrodes and their radii.
4. For cylindrical and spherical electrodes, *Paschen*'s (1889) curves and Stoletov's points become surfaces and curves, respectively. However, they still obey the same scalability law first introduced by *Paschen* (1889).
5. Critical voltages occur near pd and $pR \simeq 0.5\,\mathrm{cm{\cdot}Torr}$, suggesting easier initiation around moderately blunt objects (*Moore et al.*, 2000).

References

ICRU (1984), Stopping Powers for Electrons and Positrons, in *ICRU Rep.*, vol. 37, edited by ICRU, International Commission on Radiation Units and Measurements, Bethesda, MD, Tables 8.1 and 12.4.

Justh et al. (2010), Updating Mars-GRAM to increase the accuracy of sensitivity studies at large optical depths, in *COSPAR Scientific Assembly, COSPAR Meeting*, vol. 38, p. 4.

Leslie (2008), Earth Global Reference Atmospheric Model 2007 (Earth-GRAM07), in *COSPAR Scientific Assembly, COSPAR Meeting*, vol. 37, p. 1748.

Moore et al. (2000), Measurements of lightning rod responses to nearby strikes, *Geophys. Res. Lett.*, *27*(10), 1487–1490, doi:10.1029/1999GL011053.

Paschen (1889), Über die zum Funkenübergang in Luft, Wasserstoff und Kohlensäure bei verschiedenen Drucken erforderliche Potentialdifferenz, *Ann. Phys.*, *273*(5), 69–96, doi:10.1002/andp.18892730505.

Pasko (2006), Theoretical Modeling of Sprites and Jets, in *Sprites, Elves and Intense Lightning Discharges*, vol. 225, edited by M. Füllekrug, E. A. Mareev, and M. J. Rycroft, pp. 253–311, Kluwer Academic Publishers, Heidelberg, Germany, doi:10.1007/1-4020-4629-4_12.

Raizer (1997), *Gas Discharge Physics*, 460 pp., Springer, New York, NY.

Riousset et al. (2020), Scaling of conventional breakdown threshold: Impact for predictions of lightning and TLEs on Earth, Venus, and Mars, *Icarus*, *338*, 113,506, doi:10.1016/j.icarus.2019.113506.

Townsend (1900), The conductivity produced in gases by the motion of negatively-charged ions, *Nature*, *62*(1606), 340–341, doi:10.1038/062340b0.

von Engel and Steenbeck (1932), *Elektrische Gasentladungen: Ihre Physik und Technik*, vol. 1: Grundgesetze, 248 pp., Springer, Berlin.

von Engel and Steenbeck (1934), *Elektrische Gasentladungen: Ihre Physik und Technik*, vol. 2: Entladungseigenschaften, Technische Anwendungen, 352 pp., Springer, Berlin.

Yair (2012), New results on planetary lightning, *Adv. Space Res.*, *50*(3), 293–310, doi: 10.1016/j.asr.2012.04.013.

Acknowledgements

JAR acknowledges support from the NSF under CAREER grant 2047863 to Florida Institute of Technology.